



Published in final edited form as:

Hepatology. 2012 October ; 56(4): 1300–1310. doi:10.1002/hep.25797.

Specific bile acids inhibit hepatic fatty acid uptake

Biao Nie^{*}, Hyo Min Park^{*}, Melissa Kazantzis^{*}, Min Lin[&], Amy Henkin^{*}, Stephanie Ng^{*}, Sujin Song^{*}, Yuli Chen^{*}, Heather Tran^{*}, Robin Lai^{*}, Chris Her[#], Jacquelyn J. Maher[#], Barry M. Forman[&], and Andreas Stahl^{*}

^{*}Department of Nutritional Science and Toxicology, University of California Berkeley, Berkeley, CA 94720

[#]Department of Medicine and Liver Center, University of California San Francisco, 1001 Potrero Ave., San Francisco, CA 94110

[&]Diabetes Center, City of Hope, 1500 East Duarte Road, Duarte, CA 91010

Abstract

Bile acids are known to play important roles as detergents in the absorption of hydrophobic nutrients and as signaling molecules in the regulation of metabolism. Here we tested the novel hypothesis that naturally occurring bile acids interfere with protein-mediated hepatic long chain free fatty acid (LCFA) uptake. To this end stable cell lines expressing fatty acid transporters as well as primary hepatocytes from mouse and human livers were incubated with primary and secondary bile acids to determine their effects on LCFA uptake rates. We identified ursodeoxycholic acid (UDCA) and deoxycholic acid (DCA) as the two most potent inhibitors of the liver-specific fatty acid transport protein 5 (FATP5). Both UDCA and DCA were able to inhibit LCFA uptake by primary hepatocytes in a FATP5-dependent manner. Subsequently, mice were treated with these secondary bile acids *in vivo* to assess their ability to inhibit diet-induced hepatic triglyceride accumulation. Administration of DCA *in vivo* via injection or as part of a high-fat diet significantly inhibited hepatic fatty acid uptake and reduced liver triglycerides by more than 50%. In summary, the data demonstrate a novel role for specific bile acids, and the secondary bile acid DCA in particular, in the regulation of hepatic LCFA uptake. The results illuminate a previously unappreciated means by which specific bile acids, such as UDCA and DCA, can impact hepatic triglyceride metabolism and may lead to novel approaches to combat obesity-associated fatty liver disease.

Keywords

Fatty acid uptake; bile acids; hepatosteatosis; fatty acid transport proteins

Introduction

Bile acids contribute to several essential functions including cholesterol catabolism and intestinal lipid emulsification. In addition to their role as detergents, bile acids can also act as endocrine signaling molecules via activation of nuclear receptors, including FXR and PXR (1), as well as the G-protein coupled receptor TGR5 (1) to achieve profound effects on hepatic lipid and glucose metabolism (2).

Following their release from the gall bladder, the majority of bile acids are re-absorbed unchanged. However, secondary bile acids can be generated by intestinal bacterial species in the intestine through chemical modification of bile acids, including deconjugation, oxidation of hydroxyl groups (at C-3, C-7, and C-12), and 7 α / β -dehydroxylation (1), and can also be transported to the liver via the portal vein.

Secondary bile acids may have both detrimental and cell protective effects (3). Particularly, the human secondary bile acid ursodeoxycholic acid (UDCA) has been found to have applications for clinical use (4). UDCA is a major component of bear bile, which has been used extensively in traditional Chinese medicine for liver ailments (5). It is currently employed in the clinical treatment of diverse hepatobiliary disorders including primary biliary cirrhosis (6), primary sclerosing cholangitis (7), cystic fibrosis associated liver disease (8), and cholelithiasis (4).

Subsequent to intestinal absorption, hepatic transport systems mediate the uptake of both bile acids (9) and hydrophobic nutrients such as dietary LCFAs (10) from the circulation. We have previously demonstrated that two members of the LCFA transport protein (FATP) family of membrane proteins, FATP2 and FATP5, are important for normal hepatic LCFA uptake as well as the development of diet-induced hepatosteatosis (11–14). To identify potential FATP inhibitors we developed a high-throughput-compatible homogeneous screening method (15) that was subsequently used in proof of concept screens of a limited number of compounds against human FATP5 (16). Interestingly, this screen identified a bile acid as a weak inhibitor of FATP5.

Prior findings have hinted at an unexpected link between bile acids and hepatic FATPs. Overexpression studies with hepatic FATPs have shown that they not only enhance LCFA uptake (11) but also activate the primary bile precursors, 3 α ,7 α -dihydroxy-5 β -cholestanic acid (DHCA) and 3 α ,7 α ,12 α -trihydroxy-5 β -cholestanic acid (THCA) as well as deconjugated secondary bile to bile acid-CoA derivatives (17). We subsequently generated FATP5-null animals (11) and confirmed that they display an increase in unconjugated bile acids (14).

However, whether these dual FATP functions exist in parallel or influence each other is unclear. Particularly, whether and how bile acids can interact with the protein-mediated uptake of LCFAs by the liver has remained largely unknown. To address this potentially important link between sterol and LCFA metabolism we systematically tested for the ability of primary and secondary bile acids to inhibit FATP2- and FATP5-mediated LCFA uptake and identified secondary bile acids as potent inhibitors of LCFA uptake in vitro and in vivo.

Materials and Methods

Micro plate based LCFA uptake assays

LCFA uptake assays were based on the modification of the previously published quencher technique (15). Briefly, stable cells were plated in 96-well black wall/clear-bottom plates (Costar) in 100 μ l of DMEM/FBS for a density of 30,000–50,000 cells/well. Mouse primary hepatocytes were isolated and plated in 24-well collagen coated plates (150,000 cells/well) in 2 ml DMEM/FBS complemented with 1% 100x insulin-transferrin-selenium solution (Gibco #41400-045). Stable cells and primary hepatocytes in the plates were incubated overnight resulting in 50–70% confluency. All bile acids were dissolved in DMSO as stock solutions and then diluted with 1 \times Hank's balanced salt solution (HBSS) with 20 mM HEPES buffer, 4.5g/L glucose and 0.1% fatty acid free bovine serum albumin (HBSS BSA buffer). For 96-well and 24-well plates, 100 μ l or 1ml of HBSS BSA buffer with/without bile acids was added, respectively, to the cells followed by a 30 min incubation in 5% CO₂. The

buffer was then removed from the cells. For inhibitor screen assays, BODIPY-FA quencher mix (4.5g/L glucose HBSS, 0.1% BSA, 2 μ M fluorescently labeled LCFA C₁-BODIPY-C₁₂, 2 mM of the quencher AR 112: 760.58) with the bile acid was added. For inhibition reversibility assays, the cells were rinsed at this time point twice with PBS, followed by addition of the pre-warmed BODIPY-FA quencher mix to the cells without any bile acids. For all assays, immediately following the addition of the BODIPY-LCFA quencher mix, BODIPY-FA uptake was determined in real time using by exciting and reading fluorescence from the bottom of plates. To this end, a Gemini plate reader was set to bottom read, highest sensitivity, excitation of 488nm, and emission 515nm (with a filter cutoff at 495 nm). Readings were taken at 2-minute intervals for 2 hours and uptake velocities were calculated based on linear regression through the data points.

Animal Experiments

The generation of FATP5 null mice has been described previously (11, 14). Mice were fed standard chow prior to the high-fat diet experiments (60% calories from fat, S3282 Bio Serv). All experiments were performed with individually housed animals. For the bile acid injection experiments mice were injected subcutaneously with 3.2mg/kg DCA or LCA in 20 μ l DMSO on the back above the right hip once a day for 7 weeks while consuming a high-fat diet. For bile acid feeding experiments 5mg/g UDCA, 0.5mg/g DCA or 0.5mg/g LCA in high fat food were mixed. The mice were fed the supplemented high fat diet for 7 weeks. Their food intake and body weight were recorded once a week. During this time, the mice had ad libitum access to water and high fat food. For tissue and plasma collection, mice were fasted 4 hours prior to euthanization. After euthanasia by CO₂ asphyxiation, subcutaneous injection sites were examined to verify that no bile acid precipitates had accumulated. Liver and other organs were removed, lysed and the protein and TAG concentrations of organ lysates were assayed using the BCA protein assay kit and infinity TAG kit respectively (Thermo scientific). All procedures were approved by the UC Berkeley ACUC.

Non-radioactive in vivo hepatic LCFA uptake assay

Animals were injected subcutaneously with a dose of 6.4mg/kg body weight DCA or TCA prepared in 40 μ l DMSO at 5 pm. The mice were then fasted overnight. At 10am the following day, the mice were anesthetized with isoflurane and were given i.p. injections of 100 μ l of a 6.4mg/kg DCA or TCA solution (dissolved in a 3/2 mixture of PBS/DMSO). This was followed immediately with another i.p. injection with 20 μ M C₁-BODIPY-C₁₂ bound to 1% BSA in 100 μ l PBS. Mice were euthanized 20 minutes after the injection. Livers were harvested, weighed, and homogenized in 2ml RIPA buffer.

Protein concentrations of the homogenized samples were assayed using a BCA assay kit and the remaining lysates were extracted with 3 volumes of Dole's reagent (heptane: 2-propanol: 2N sulfuric acid=10:40:1 v/v/v). Following centrifugation at 18,000 g for 10 min, the clear organic-phase supernatant (top layer) was collected. 50 μ l of the supernatant was added to a 96-well plate and fluorescence at 488nm excitation, 515nm emission was determined. The fluorescence units were normalized to either protein concentrations or organ weights.

Statistical Analysis

The average of data and standard error of mean are shown in the figures. Statistical significance was determined by using a Student's t-test, one-way, or two-way ANOVA as appropriate.

Please see the Supplemental Material Section for further Material and Method information.

Results

We generated stable HEK-293 based cell lines following transfection of the cells with human FATP2, FATP5, or empty expression constructs. Utilizing a quencher-based real time uptake assay (15), we were able to determine the correlation between FATP expression (Sup. Fig. 1A insert) and LCFA uptake rates (Sup. Fig. 1A). After optimization of uptake conditions (see Material and Methods) linear regression of fluorescent values showed a significant increase in the Bodipy-LCFA (C1-Bodipy-C12) uptake rate in FATP5 (132fold) and FATP2 (70fold) expressing cells over vector controls, thus giving us a robust signal to background ratio for inhibitor screens. Bodipy-LCFA uptake was also visualized following uptake assays and showed intracellular accumulation of the fatty acid probe in intracellular structures with the morphological appearance of ER and small lipid droplets (Sup. Fig. 1B). This is in line with previous reports of Bodipy-LCFA uptake. C1-Bodipy-C12 fatty acids have been used extensively to study long-chain fatty acid uptake (for examples see (18–20)) and their uptake can be competed with unlabeled fatty acids (15) arguing that it utilizes the same transporters. Also, bodipy-fatty acids can become incorporated into cellular lipids (21).

We initially screened for the effects of the most common conjugated and unconjugated primary bile acids, i.e. cholic acid (CA), taurocholic acid (TCA), chenodeoxycholic acid (CDCA) and taurochenodeoxycholic (TCDCA). While conjugated primary bile acids did not reduce LCFA uptake (Fig. 1–2), both CA and CDCA specifically inhibited FATP5-mediated LCFA uptake (Fig. 1–2) with IC_{50} s in the low micro molar range (Tab. 1). XTT assays demonstrated that none of the bile acids were toxic in the concentration range tested (Fig. 1–2). Interestingly, FATP5 inhibition by CA and CDCA showed complete reversibility (Sup. Fig. 2). A brief rinse of the cells treated with the bile acids was able to remove the inhibitory effect immediately. This pattern of inhibition was consistent with the hypothesis that bile acids which can serve as substrates for enzymatic activation by FATPs can inhibit LCFA uptake. To corroborate this notion, we tested the effect of the FATP2 and -5 substrate THCA, which was predicted to be a potent inhibitor of both FATPs. However, the addition of THCA resulted only in weak inhibition (FATP5) or no inhibition (FATP2) of LCFA uptake rates (Sup. Fig. 3B). Also, alpha-muricholic acid, one of the predominant unconjugated bile acids in mice, had no effect on LCFA uptake (Sup. Fig. 3A).

To compare these findings to those of previously published inhibitors of FATP2 (22), FATP2- and FATP5-overexpressing cells were treated with compounds CB-2 ((5E)-5-[(3-bromo-4-hydroxy-5-methoxyphenyl)methylene]-3-(3-chlorophenyl)-2-thioxothiazolidin-4-one), CB-5 (2-benzyl-3-(4-chlorophenyl)-5-(4-nitrophenyl)-1H-pyrazolo[5,1-b]pyrimidin-7-one), and CB-6 (2-[7-(trifluoromethyl)-2,3-dihydro-1H-1,4-diazepin-5-yl]naphthalen-1-ol) (Sup. Fig. 4). All three compounds inhibited FATP2 mediated LCFA uptake with IC_{50} s of 8 μ M, 18 μ M, and 12 μ M, respectively. CB-5 (7 μ M) and CB-6 (38 μ M) also showed inhibition of FATP5 mediated uptake although it should be noted that CB-5 elicited marked cytotoxicity (Sup. Fig. 4). Interestingly, inhibition by CB-6 but not CB-2 was irreversible, hinting at a different inhibition mechanism from that of the bile acids (Sup. Fig. 2).

Next, we expanded our screening to the secondary bile acids ursodeoxycholic acid (UDCA), tauroursodeoxycholic acid (TUDCA), deoxycholic acid (DCA), and lithocholic acid (LCA). While TUDCA did not inhibit FATP2 and -5 mediated uptake, UDCA was identified as a potent inhibitor of FATP5 (Fig. 3) with an IC_{50} of 5 μ M (Tab. 1).

An even more potent inhibition of FATP5 and, to a lesser degree, of FATP2 was observed following DCA addition (Fig. 4) with IC_{50} s of 0.19 and 5 μ M, respectively. While DCA is a naturally occurring secondary bile acid, it is also known to have cytotoxic effects particularly at a higher concentration. Importantly, DCA did not display any cytotoxicity

within the FATP5 inhibitory range (Fig. 4) and inhibition was found to be reversible (Sup. Fig. 2). In contrast, taurodeoxycholic acid (TDCA) inhibited neither FATP2 nor FATP5 mediated LCFA uptake (data not shown). Another naturally occurring secondary bile acid, LCA, showed no inhibition of LCFA uptake mediated by either FATP5 or FATP2 (Fig. 4).

To further explore the physiological and pharmacological implications of hepatic FATP inhibition by secondary bile acids we tested the effects of UDCA on LCFA uptake by primary hepatocytes. Using a FACS-based LCFA uptake assay that allows for the gating of viable cells (11), we found that UDCA but not TUDCA inhibited LCFA uptake by primary human hepatocytes (Sup. Fig. 5). UDCA also inhibited LCFA uptake by primary mouse hepatocytes from C57Bl/6 animals without any detectable cytotoxic effects (Fig. 5A right). Importantly, this effect was entirely FATP5 dependent, as UDCA failed to inhibit LCFA uptake by primary hepatocytes from FATP5-null animals (Fig. 5A). As predicted from our stable cell line results, the secondary bile acid DCA inhibited hepatocyte LCFA uptake significantly (Fig. 5B) while LCA showed no inhibition of LCFA uptake by primary mouse hepatocytes (Fig. 5D). Further, DCA mediated inhibition was not associated with toxicity (Fig. 5B right) and, importantly, was primarily dependent on FATP5 as the effect was abolished in FATP5-null hepatocytes (Fig. 5B). We confirmed DCA inhibition of fatty acid uptake by primary hepatocytes using ^{14}C -labeled oleate (Sup. Fig. 6). Subsequent assays focused on the uptake of radiolabeled metabolites by primary hepatocytes and demonstrated that DCA can inhibit the uptake of a wide range of fatty acids without affecting uptake of a 2-deoxy-D- ^3H glucose/glucose mix (Fig. 5C).

Next we thought to determine the *in vivo* effects of the most potent bile acid, DCA. To this end, LCA and DCA were injected into animals both acutely and chronically and the resulting effects on hepatic LCFA uptake and TAG accumulation respectively were measured. To this end we established an *in vivo* assay of acute hepatic LCFA uptake based on the injection of a fluorescent fatty acid analog (C1-Bodipy-C12) followed by extraction of hepatic lipids 20 min post injection. Using this approach we were able to reproduce *in vivo* the ~50% reduction in hepatic LCFA uptake in FATP5 null animals (Fig. 6A) previously only shown with isolated hepatocytes and ^{14}C -oleate (11). We utilized this novel assay in conjunction with concomitant bile acid injections to establish *in vivo* a dose-response curve for DCA (Fig. 6B). As predicted from our cell based studies, the inhibitory effect was observed with DCA but not TCA (Fig. 6C). Importantly, DCA inhibition was abolished in FATP5 KO mouse hepatocytes (Fig. 6C). To determine the chronic effects of DCA on hepatic lipid accumulation, we used an intermediate dose (3.2 mg/kg) from our titration experiment and injected mice with DCA, LCA or vehicle (DMSO) for 47 days while the animals were fed a high-fat diet. This injection routine neither triggered an increase in respiration (Fig. 6D) nor did it affect food consumption or body weight (Fig. 6E and Sup. Fig. 7A). DCA treatment did, however, have a profound effect on hepatic triglyceride accumulation. DCA caused a 68% reduction (6.6 vs. 2.1 mg TAG/g protein) in the triglyceride content of the liver (Fig. 6F). As predicted from the lack of DCA inhibition of FATP5-null primary hepatocytes, DCA injections of FATP5-null animals did not cause a further reduction in liver TAG (Fig. 6F) beyond the effect of FATP5 deficiency by itself, which reduced diet-induced hepatic triglyceride accumulation by about 50% (11).

In order to choose a more physiological delivery route for DCA and to assess in more detail the effect of this secondary bile acid on liver function we supplemented high fat diets with DCA. In pilot experiments we determined that DCA addition in the range of 0 to 0.2% caused a dose dependent reduction in acute liver LCFA absorption without causing a detectable increase in circulating liver enzymes (Fig. 7A). Based on these results we chose the lowest effective DCA dose (0.05%) for a 7 week high-fat diet induced hepatosteatosis study. Neither DCA nor LCA feeding resulted in changes in respiratory rate (Sup. Fig. 7C),

caloric output over a 36h period (Sup. Fig. 7B), food intake, or body weight (Sup. Fig. 7D–E). Further, circulating lipids in the form of TAG and cholesterol were unchanged by dietary DCA supplementation in the range from 0.03%–0.4% (Sup. Fig. 7F–G). Notably, 0.05% DCA, but not LCA, supplementation resulted in an approximately 50% reduction in hepatic TAG content (Fig. 7B) and markedly reduced lipid droplets in BODIPY-stained liver sections (Fig. 7D). Importantly, DCA treatment did not lead to hepatotoxicity or fibrosis based on ALT/AST assays (Fig. 7C) and liver morphology (Sup. Fig. 8). To address potential inhibition of intestinal LCFA transporters by bile acids we determined that neither DCA, UDCA, nor LCA inhibited the principal intestinal fatty acid transporter FATP4 (23) (Sup. Fig. 9A–C). Further, direct measurements of intestinal fatty acid absorption with fat tolerance tests determined that the appearance of a labeled fatty acid in the circulation was not suppressed by DCA supplementation (Sup. Fig. 9D). Lastly, we addressed the ability of DCA and LCA to activate hepatic FXR target genes using quantitative PCR analysis and found that both secondary bile acids were FXR activators that suppressed *Cyp7a1* mRNA levels to a comparable degree (Sup. Fig. 10).

Discussion

Our understanding of the physiological importance of bile acids for human health has been greatly expanded over the last decade and revealed new roles for bile acids as regulators of nuclear receptors and metabolic rates (24). Bile acids regulate the enterohepatic recirculation and inhibit the expression of rate limiting bile acid synthesis genes such as *Cyp7a1* (25) via activation of the nuclear hormone receptors farnesoid X receptor alpha (FXR-alpha) (26, 27) and increased expression of the short heterodimer partner (SHP) (28) which in turn can down-regulated hepatic fatty acid and triglyceride biosynthesis (29). Bile acids can also activate the heterotrimeric G-protein receptor TGR5, which has been demonstrated to be involved in the regulation of glucose and energy homeostasis (30). For example, CA has been shown to trigger the TGR5–cAMP–D2 signalling pathway and to enhance oxygen consumption independently of FXR-alpha in vivo (24). Here we report a novel link between bile acids and metabolism, i.e. the ability of, specific bile acids such as DCA and UDCA to inhibit hepatic LCFA uptake.

Other bile acids, including CA and CDCA, showed inhibition only at slightly supraphysiological levels based on circulating serum bile acid levels (31, 32). However, postprandial bile concentrations in the portal vein may be significantly higher and thus result in decreased hepatic LCFA uptake. While chylomicron remnant uptake via endocytosis is thought of as the classical contributor to postprandial hepatic TAG uptake, inhibition of FATP5 has been shown to lead to a reduction in hepatic postprandial LCFA uptake, a redistribution of dietary lipids away from the liver, and reduced susceptibility to diet-induced hepatosteatosis (10). Thus, one could speculate that one possible physiological function for this FATPs inhibition could be to channel dietary LCFA to adipose stores in the postprandial phase when bile acid levels are high, but allow for maximal LCFA uptake to support ketogenesis during fasting conditions when LCFA are released by adipose tissue and circulating bile acid levels are low.

A particularly potent inhibitor of hepatic fatty acid transporters was the secondary bile acid DCA. DCA's inhibitory effect occurred at nM concentrations well below the limit for cytotoxicity and was not only observed in cell lines and primary cells but also in vivo where DCA injections and feeding lowered hepatic TAG content in the context of high fat induced hepatosteatosis by 50–70% and acutely reduced hepatic LCFA uptake by 31%. Notably, the secondary bile acid LCA, which did not inhibit FATP5/2 dependent cellular LCFA uptake, had no effect on liver TAG content or in vivo hepatic LCFA uptake. Clearly, bile acids can impact fatty liver disease through multiple mechanisms including FXR and TGR5

activation. However, we would argue that the anti-steatotic effects of DCA are, at least in part, due to its novel function as FATP5 inhibitor. This assertion is based on several lines of evidence. The facts that LCA and DCA activate TGR5 equally (33, 34) while only DCA lowered hepatic TAG as well as the lack of enhanced respiratory rates following DCA injections or feeding make a primary involvement of TGR5 unlikely. Secondly, both DCA and LCA activated FXR based on suppression of Cyp7a1 expression but differed in their effect on hepatosteatosis. Thirdly, DCA treatment did not inhibit intestinal FATP4 nor did it reduce intestinal lipid absorption (Sup. Fig. 9) or cause hepatotoxicity (Fig. 7C–E). In contrast, DCA, but not LCA, inhibited LCFA uptake by primary hepatocytes in an FATP5 dependent fashion and DCA injections were able to reduce the acute hepatic fatty acid uptake in vivo in a dose dependent fashion (Fig. 6B). Lastly, and potentially most importantly, DCA's anti-steatotic effects were not observed in FATP5KO animals, which recapitulates our findings from isolated hepatocytes, and supports the model that inhibition of transporter-mediated hepatic LCFA uptake plays a key role in the prevention/reversion of diet-induced hepatosteatosis.

Physiological concentrations of DCA have been reported to be between 0.133 (31)-0.415 μM (32), placing it well within the observed IC_{50} 0.19 μM for FATP5. DCA is the only bile acid that has an IC_{50} within its physiological range. Importantly, as DCA is the product of specific bacterial strains in the colon (35), predominantly belonging to the genera Eubacterium and Clostridium (36), changes in bacterial composition (37) and/or antibiotic use (38) would be predicted to impact hepatic LCFA absorption.

While the physiological levels of UDCA in humans are likely to be too low (~54 nM (32)) to impact hepatic LCFA uptake, oral UDCA administration has been widely used in the clinic for the treatment of several hepatobiliary disorders including non-alcoholic steatohepatitis (NASH). While passage through the enterohepatic circulation can lead to the reconjugated and bioconversion, we expect that with chronic administration of DCA or UDCA we can establish a mix of conjugated and unconjugated bile acids. Indeed this has been shown for UDCA treatment in gallstone patients (39) and, importantly, feeding of DCA and UDCA supplemented diets has been shown to increase levels of both conjugated as well as unconjugated forms of these bile acids (40). Oral administration of UDCA can also raise circulating UDCA levels to over 17 μM (41), which is well above the observed IC_{50} for FATP5. Our mechanistic understanding of UDCA actions is incomplete but possibly could include increased hydrophilicity of bile (3), inhibition of apoptosis (3), and conjugation to TUDCA, which has been shown to reduce ER stress in fatty liver disease animal models (42). Here we show a potential novel mechanism by which UDCA might inhibit LCFA uptake through blockade of FATP5. We were able to show that UDCA inhibited hepatocyte LCFA uptake in an FATP5 dependent fashion. In comparison, results from human studies using UDCA to lower hepatosteatosis and NASH showed that the administration of UDCA over 2 years at a dose of 13–15 mg/kg/day to 166 patients did not produce an effective result as compared to placebo (43). Results from another study indicated that administration of a high dose of UDCA (23–28 mg/kg/day) for 18 months to 185 NASH patients failed to improve the overall histology but significantly improved lobular inflammation in males, younger patients (up to 50 years of age), slightly overweight patients, and in patients with hypertension (44). We would suggest that oral UDCA, similarly to DCA, acts at least in part by blocking hepatic uptake of free fatty acids and thus would predict that UDCA has a more pronounced effect in reducing the hepatic LCFA uptake in patients with high fat or high protein.

While we present here clear data in support of the idea that select bile acids such as DCA can inhibit FATP5, the underlying structure/function relationships and biochemical mechanisms of inhibition will require further study. Besides the point that none of the tested

conjugated bile acids inhibited FATP5 or -2, no clear lead compound structure emerged from the tested molecules. Further, while FATP5 can act as a bile-CoA ligase (14), we found no support for the hypothesis that all bile acids that are potentially activated to bile acid-CoA by FATP5 or -2 are inhibitors of LCFA uptake based on the lack of inhibition by THCA and LCA, which would be predicted to be substrates for FATP2/5 and FATP5, respectively (14, 17). Based on the rapid reversibility of inhibition, the lack of bile acid transporters in HEK-293 cells (45) (46) and the absence of TGR5 (47), and FXR (48) in these cells, it is likely that the bile acids do not enter or signal in HEK-293 and rather act on the extracellular domain of FATP5/2 as competitive inhibitors. Alternatively, FATP5 could have a dual function as a high affinity transporter for a specific subset of bile acids, overlapping with the pattern of inhibition. Clearly, further studies are needed to test this exciting possibility.

In summary, we have shown that the secondary bile acids UDCA and DCA are potent suppressors of hepatic LCFA uptake via reversible inhibition of FATP5. Based on this novel observation we can make several interesting predictions including a new mode by which intestinal bacterial composition and activity may influence hepatic lipid metabolism and that the clinical use of UDCA for the treatment of non-alcoholic fatty liver disease would be more beneficial if the disorder is driven by hepatic uptake, rather than de novo synthesis, of LCFAs.

Supplemental Methods

Bile acids and chemicals

All bile acids were purchased from Sigma except for Muricholic acid and THCA, which were provided by Dr. Barry Forman. The compounds CB-2 ((5E)-5-[(3-bromo-4-hydroxy-5-methoxyphenyl)methylene]-3-(3-chlorophenyl)-2-thioxothiazolidin-4-one), CB-5 (2-benzyl-3-(4-chlorophenyl)-5-(4-nitrophenyl)-1H-pyrazolo[5,1-b]pyrimidin-7-one), and CB-6 (2-[7-(trifluoromethyl)-2,3-dihydro-1H-1,4-diazepin-5-yl]naphthalen-1-ol) were purchased from NCI's Developmental Therapeutics Program (DTP). The fluorescent long-chain fatty acid analog 4,4-difluoro-5-methyl-4-bora-3a,4a-diaza-s-indacene-3-dodecanoic acid (C1-BODIPY-C12 500/510, Cat# D3823) and 4,4-difluoro-1,3,5,7,8-pentamethyl-4-bora-3a,4a-diaza-s-indacene (BODIPY® 493/503 for lipid staining, Cat# D3922) were purchased from Invitrogen. The quencher dye AR 112: 760.58 was provided by Molecular Devices. ALT and AST assay kits were from Bio-Vision. Trichrome staining kit was purchased from Sigma.

Purity of bile acids

Purity: Cat#U5127 UDCA >99%, Cat# TUDCA>95%, Cat# C1129 CA>98%, Cat# T4009 TCA>95%, Cat# D2510 DCA>99%, Cat# T0875 TDCA>95%, Cat# L6250 LCA>97%, Cat# C9377 CDCA>97%, Cat# T6260 TCDCA>95%

Cell lines and tissue culture

Human embryonic kidney 293 cell lines were constructed to stably express human recombinant hsFATP4, hsFATP5, hsFATP2 and the vector control cells have been described previously (11, 13). Cells were grown in Dulbecco's Modified Eagle Medium (Gibco Invitrogen, Carlsbad, CA), containing 4.5g/L D-glucose and supplemented with 10% fetal bovine serum (FBS), 1 mg/ml gentamicin, 4mM L-glutamine, 100 units/ml penicillin, 100µg/ml streptomycin, 1 mg/ml G418.

Western blots

Polyclonal antibodies against murine FATP5 and FATP2 were raised in rabbits as previously described (11, 13) and were 1:500 diluted in 1% non-fat milk before using. Anti- α -Tubulin (11H10,#2125) Rabbit monoclonal antibody and secondary antibodies from Cellsignaling and LI-COR were 1:1000 or 1:10000 diluted respectively before using.

Isolation of mouse hepatocytes

For isolating the murine primary hepatocytes, the portal vein of mice were cannulated and perfused for 4 minutes at 12ml/minute with pre-warmed perfusion buffer (Gibco Invitrogen, Carlsbad, CA). Buffer was subsequently replaced with collagenase buffer (Gibco Invitrogen, Carlsbad, CA) for approximately another 6 minutes until tissue was completely digested. The liver was removed and rinsed in perfusion buffer. The suspension was passed through a nylon mesh sieve. Mouse hepatocytes viability was check by trypan blue exclusion and cells were plated in 24-well collagen coated plates (150,000 cells/well) in 2 ml DMEM/FBS complemented with 1% 100x insulin-transferrin-selenium solution (Gibco #41400-045).

XTT assay

293 cells in 200 μ l DMEM/FBS were added to the 96-well plate or primary hepatocytes in 2ml DMEM/FBS were added to a 24-well collagen coated plate, marking a density of 150,000 cells/well or 6000–8000 cells/well respectively. The plates were then incubated in 5% CO₂ overnight. Following the first incubation, the indicated bile acid or DMSO control was added. After an additional 48 hours of incubation, the cells were assayed with a XTT kit (ATCC) according to the manufacturer's instructions.

Fluorescence-activated cell sorter (FACS)-based LCFA uptake assays

Primary human hepatocytes (Zen-Bio) were suspended and treated with 10 μ M or 100 μ M UDCA or TUDCA in 3ml DMEM at 37°C, 5% CO₂ for 30 minutes. LCFA uptake assays were performed as previously described (11, 49). Briefly, C1-BODIPY-C12 bound to 0.1% BSA was added at final concentration 2 μ M, followed the incubation at 37 °C, 5% CO₂ for 30 minutes. Then, tubes were put on ice immediately to stop the uptake reaction. Following centrifuge at 4°C, 0.5ml cold PBS was added in the cell and they were vortexed. Just before the FACS assay, 0.5 μ l propidium iodide (PI) was added. Avarage C1-BODIPY-C12 fluorecence of 5000 viable (PI negative) cells was determined using histogram plots. Overall viability was determined from the ratio of PI-egative to PI-positive cells.

Non-radioactive intestinal in vivo LCFA absorption assay

Mice were gavaged with 200 μ l of an olive oil/20 μ M BODIPY-FFA mixture containing 0% or 0.05% DCA. Blood samples were drawn at 0, 30, 60, 120 and 240 minutes post gavage and the fluorescences of the serum samples at 515 nm was determined using a plate reader.

Staining of neutral lipids with BODIPY (500/510)

Fresh frozen liver sections were stained with BODIPY to visualize neutral lipid droplets as reported before (50). Briefly, livers from mice were fixed with paraformaldehyde (PFA) (4% PFA in PBS) for 60 min at room temperature, cryopreserved, blocked and frozen sectioned. For BODIPY fluorescence staining, slides with liver sections were rinsed twice with PBS. The slides were stained with BODIPY 493/503 (10 μ g/ml in PBS) working solution for 2 hours at room temperature and then rinsed twice with PBS and mounted with a DAPI containing mounting medium.

293 cells for microscopy experiments were grown on glass coverslips in 6 well plate. BODIPY (D3823, Molecular Probes, USA) was diluted in PBS DMSO at a concentration of

1mg/mL and applied to cells for 1hr. We fixed cells in 4% paraformaldehyde for 30mins on the ice and used 4,6-diamidino-2-phenylindole (DAPI) to identify nuclei. Following fixation, cells were washed 3 times in cold phosphate-buffered saline (PBS). Digital images were obtained with a Zeiss710 confocal laser scanning microscope.

Mason's trichrome staining

Masson's trichrome stains were performed according to the kit's manufacturer's instructions (Sigma).

Serum lipid assays

Serum for lipid assays was collected after 1 week DCA-high fat feeding. Total cholesterol and TAG were estimated by use of commercially available cholesterol assay kit (Stanbio, USA) and TAG assay kit (Thermo scientific, USA).

Uptake assay of radiolabeled compounds

Mouse primary hepatocytes were provided by UCSF liver center and all radioactive materials were purchased from American Radiolabeled Chemicals, Inc. (ARC). Cells were seeded in collagen coated 24-well plates for uptake assay. 24 hrs after seeding, cells were treated without or with DCA (5 μ M) for 30 min at 37°C, and each fatty acid (Arachidonic acid [5,6,8,9 11,12,14,15-³H(N)], Oleic acid [1-¹⁴C], Palmitic acid [1-¹⁴C], Octanoic acid [1-¹⁴C]) (all fatty acids were at a final concentration of 20 μ M, 0.5 μ Ci activity) and 2-deoxy-D-[³H]glucose/glucose mix (10 nmol/0.5 μ Ci of 2-deoxy-D[³H]glucose mixed with unlabeled glucose to yield a final concentration of 1mM) were then added to initiate the uptake reaction. After 45 min, the cells were washed 3 times with ice-cold PBS and solubilized in 0.2 ml of RIPA buffer. Radiolabeled compounds uptake by cells was measured in 4 ml of scintillation fluid by using a Beckman LS6500 scintillation counter. Each fatty acid and glucose uptake is presented from the mean of multiple experiments.

Metabolic Chamber Assays

Metabolic rates of animals were determined as previously described (50). VO₂ and VCO₂ measurements were performed in the absence of food. Averages were calculated using periods of no animal movement.

qRT-PCR

Total RNAs were isolated from mouse livers with TRIzol (Invitrogen #15596). Following OD_{260/280} of RNAs were determined, reverse transcription was performed with Taqman kit by standard method. After 95°C 10 min denaturizing, the qPCRs were performed in 95°C 15 sec, 60°C 45 sec, repeated 39 cycles with SYBR Green kit (ABI). The primer sequences used are listed in supplemental table 1.

Supplementary Material

Refer to Web version on PubMed Central for supplementary material.

Acknowledgments

Financial support:

This research was supported by NIH/NIDDK grants R56DK066336 and R01DK066336 to A.S. and benefitted from the UCSF liver center grant NIH P30 DK026743.

Abbreviations

CA	cholic acid
CDCA	chenodeoxycholic acid
DCA	deoxycholic acid
DHCA	3a,7a-dihydroxy-cholestanoic acid
FACS	fluorescence-activated cell sorter
FATP	fatty acid transport protein
FBS	fetal bovine serum
LCFA	long chain free fatty acid
LCA	lithocholic acid
MA	muricholic acid
NASH	non-alcoholic steatohepatitis
RFU	relative fluorescence unit
TCA	taurocholic acid
TCDC	taurochenodeoxycholic acid
TUDCA	tauroursodeoxycholic acid
TAG	triglyceride
THCA	3a,7a,12a-Trihydroxy-5 β -cholestanoic acid
TUDCA	tauroursodeoxycholic acid
UDCA	ursodeoxycholic acid
XTT	2,3-bis-(2- methoxy-4- nitro-5-sulfohenyl)-2H-tetrazolium-5-carboxanilide

References

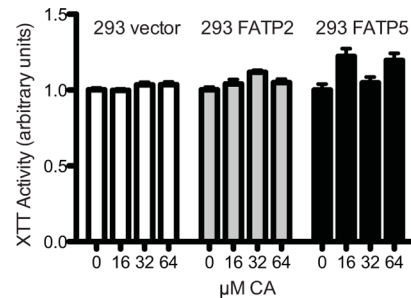
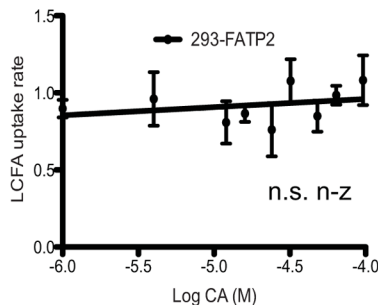
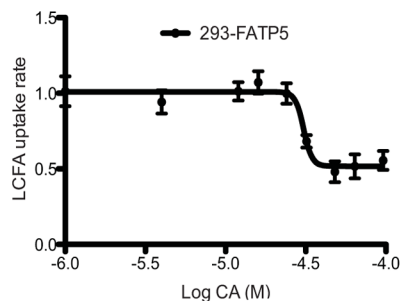
1. Hylemon PB, Zhou H, Pandak WM, Ren S, Gil G, Dent P. Bile acids as regulatory molecules. *J Lipid Res.* 2009; 50:1509–1520. [PubMed: 19346331]
2. Trauner M, Claudel T, Fickert P, Moustafa T, Wagner M. Bile acids as regulators of hepatic lipid and glucose metabolism. *Dig Dis.* 2010; 28:220–224. [PubMed: 20460915]
3. Perez MJ, Briz O. Bile-acid-induced cell injury and protection. *World J Gastroenterol.* 2009; 15:1677–1689. [PubMed: 19360911]
4. Kowdley KV. Ursodeoxycholic acid therapy in hepatobiliary disease. *Am J Med.* 2000; 108:481–486. [PubMed: 10781781]
5. Feng Y, Siu K, Wang N, Ng KM, Tsao SW, Nagamatsu T, Tong Y. Bear bile: dilemma of traditional medicinal use and animal protection. *J Ethnobiol Ethnomed.* 2009; 5:2. [PubMed: 19138420]
6. Heathcote EJ. Evidence-based therapy of primary biliary cirrhosis. *Eur J Gastroenterol Hepatol.* 1999; 11:607–615. [PubMed: 10418931]
7. Sinakos E, Lindor K. Treatment options for primary sclerosing cholangitis. *Expert Rev Gastroenterol Hepatol.* 2010; 4:473–488. [PubMed: 20678020]
8. Colombo C. Liver disease in cystic fibrosis. *Curr Opin Pulm Med.* 2007; 13:529–536. [PubMed: 17901760]
9. Dawson PA, Lan T, Rao A. Bile acid transporters. *J Lipid Res.* 2009; 50:2340–2357. [PubMed: 19498215]

10. Doege H, Stahl A. Protein-mediated fatty acid uptake: novel insights from in vivo models. *Physiology (Bethesda)*. 2006; 21:259–268. [PubMed: 16868315]
11. Doege H, Baillie RA, Ortegon AM, Tsang B, Wu Q, Punreddy S, Hirsch D, et al. Targeted deletion of FATP5 reveals multiple functions in liver metabolism: alterations in hepatic lipid homeostasis. *Gastroenterology*. 2006; 130:1245–1258. [PubMed: 16618416]
12. Doege H, Grimm D, Falcon A, Tsang B, Storm TA, Xu H, Ortegon AM, et al. Silencing of hepatic fatty acid transporter protein 5 in vivo reverses diet-induced non-alcoholic fatty liver disease and improves hyperglycemia. *J Biol Chem*. 2008; 283:22186–22192. [PubMed: 18524776]
13. Falcon A, Doege H, Fluit A, Tsang B, Watson N, Kay MA, Stahl A. FATP2 is a hepatic fatty acid transporter and peroxisomal very long-chain acyl-CoA synthetase. *Am J Physiol Endocrinol Metab*. 2010
14. Hubbard B, Doege H, Punreddy S, Wu H, Huang X, Kaushik VK, Mozell RL, et al. Mice deleted for fatty acid transport protein 5 have defective bile acid conjugation and are protected from obesity. *Gastroenterology*. 2006; 130:1259–1269. [PubMed: 16618417]
15. Liao J, Sportsman R, Harris J, Stahl A. Real-time quantification of fatty acid uptake using a novel fluorescence assay. *J Lipid Res*. 2005; 46:597–602. [PubMed: 15547301]
16. Zhou W, Madrid P, Fluit A, Stahl A, Xie XS. Development and validation of a high-throughput screening assay for human long-chain fatty acid transport proteins 4 and 5. *J Biomol Screen*. 2010; 15:488–497. [PubMed: 20448275]
17. Mihalik SJ, Steinberg SJ, Pei Z, Park J, Kim do G, Heinzer AK, Dacremont G, et al. Participation of two members of the very long-chain acyl-CoA synthetase family in bile acid synthesis and recycling. *J Biol Chem*. 2002; 277:24771–24779. [PubMed: 11980911]
18. Faergeman NJ, Di Russo CC, Elberger A, Knudsen J, Black PN. Disruption of the *Saccharomyces cerevisiae* homologue to the murine fatty acid transport protein impairs uptake and growth on long-chain fatty acids. *J Biol Chem*. 1997; 272:p8531–8538.
19. Schaffer JE, Lodish HF. Expression cloning and characterization of a novel adipocyte long chain fatty acid transport protein. *Cell*. 1994; 79:427–436. [PubMed: 7954810]
20. Hirsch D, Stahl A, Lodish HF. A family of fatty acid transporters conserved from mycobacterium to man. *Proc Natl Acad Sci U S A*. 1998; 95:8625–8629. [PubMed: 9671728]
21. Kasurinen J. A novel fluorescent fatty acid, 5-methyl-BDY-3-dodecanoic acid, is a potential probe in lipid transport studies by incorporating selectively to lipid classes of BHK cells. *Biochem Biophys Res Commun*. 1992; 187:1594–1601. [PubMed: 1417832]
22. Sandoval A, Chokshi A, Jesch ED, Black PN, Dirusso CC. Identification and characterization of small compound inhibitors of human FATP2. *Biochem Pharmacol*. 2010; 79:990–999. [PubMed: 19913517]
23. Stahl A, Hirsch DJ, Gimeno RE, Punreddy S, Ge P, Watson N, Patel S, et al. Identification of the major intestinal fatty acid transport protein. *Mol Cell*. 1999; 4:299–308. [PubMed: 10518211]
24. Watanabe M, Houten SM, Matak C, Christoffolete MA, Kim BW, Sato H, Messaddeq N, et al. Bile acids induce energy expenditure by promoting intracellular thyroid hormone activation. *Nature*. 2006; 439:484–489. [PubMed: 16400329]
25. Anakk S, Watanabe M, Ochsner SA, McKenna NJ, Finegold MJ, Moore DD. Combined deletion of *Fxr* and *Shp* in mice induces *Cyp17a1* and results in juvenile onset cholestasis. *The Journal of clinical investigation*. 2011; 121:86–95. [PubMed: 21123943]
26. Makishima M, Okamoto AY, Repa JJ, Tu H, Learned RM, Luk A, Hull MV, et al. Identification of a nuclear receptor for bile acids. *Science*. 1999; 284:1362–1365. [PubMed: 10334992]
27. Wang H, Chen J, Hollister K, Sowers LC, Forman BM. Endogenous bile acids are ligands for the nuclear receptor FXR/BAR. *Molecular cell*. 1999; 3:543–553. [PubMed: 10360171]
28. Goodwin B, Jones SA, Price RR, Watson MA, McKee DD, Moore LB, Galardi C, et al. A regulatory cascade of the nuclear receptors FXR, SHP-1, and LXR-1 represses bile acid biosynthesis. *Molecular cell*. 2000; 6:517–526. [PubMed: 11030332]
29. Watanabe M, Houten SM, Wang L, Moschetta A, Mangelsdorf DJ, Heyman RA, Moore DD, et al. Bile acids lower triglyceride levels via a pathway involving FXR, SHP, and SREBP-1c. *The Journal of clinical investigation*. 2004; 113:1408–1418. [PubMed: 15146238]

30. Thomas C, Gioiello A, Noriega L, Strehle A, Oury J, Rizzo G, Macchiarulo A, et al. TGR5-mediated bile acid sensing controls glucose homeostasis. *Cell metabolism*. 2009; 10:167–177. [PubMed: 19723493]
31. Setchell KD, Matsui A. Serum bile acid analysis. *Clin Chim Acta*. 1983; 127:1–17. [PubMed: 6337748]
32. Bentayeb K, Batlle R, Sanchez C, Nerin C, Domeno C. Determination of bile acids in human serum by on-line restricted access material-ultra high-performance liquid chromatography-mass spectrometry. *J Chromatogr B Analyt Technol Biomed Life Sci*. 2008; 869:1–8.
33. Maruyama T, Miyamoto Y, Nakamura T, Tamai Y, Okada H, Sugiyama E, Itadani H, et al. Identification of membrane-type receptor for bile acids (M-BAR). *Biochemical and biophysical research communications*. 2002; 298:714–719. [PubMed: 12419312]
34. Kawamata Y, Fujii R, Hosoya M, Harada M, Yoshida H, Miwa M, Fukusumi S, et al. A G protein-coupled receptor responsive to bile acids. *The Journal of biological chemistry*. 2003; 278:9435–9440. [PubMed: 12524422]
35. Ridlon JM, Kang DJ, Hylemon PB. Bile salt biotransformations by human intestinal bacteria. *J Lipid Res*. 2006; 47:241–259. [PubMed: 16299351]
36. Wells JE, Hylemon PB. Identification and characterization of a bile acid 7 α -dehydroxylation operon in *Clostridium* sp. strain TO-931, a highly active 7 α -dehydroxylating strain isolated from human feces. *Appl Environ Microbiol*. 2000; 66:1107–1113. [PubMed: 10698778]
37. Swann JR, Want EJ, Geier FM, Spagou K, Wilson ID, Sidaway JE, Nicholson JK, et al. Systemic gut microbial modulation of bile acid metabolism in host tissue compartments. *Proceedings of the National Academy of Sciences of the United States of America*. 2011; 108 (Suppl 1):4523–4530. [PubMed: 20837534]
38. Toda T, Ohi K, Kudo T, Yoshida T, Ikarashi N, Ito K, Sugiyama K. Ciprofloxacin suppresses Cyp3a in mouse liver by reducing lithocholic acid-producing intestinal flora. *Drug Metab Pharmacokinet*. 2009; 24:201–208. [PubMed: 19571431]
39. Hill A, Ross PE, Bouchier IA. 125I Radioimmunoassay of serum ursodeoxycholy conjugates. *Clinica chimica acta; international journal of clinical chemistry*. 1983; 127:327–336.
40. Zhang Y, Klaassen CD. Effects of feeding bile acids and a bile acid sequestrant on hepatic bile acid composition in mice. *Journal of lipid research*. 2010; 51:3230–3242. [PubMed: 20671298]
41. Sinakos E, Marschall HU, Kowdley KV, Befeler A, Keach J, Lindor K. Bile acid changes after high-dose ursodeoxycholic acid treatment in primary sclerosing cholangitis: Relation to disease progression. *Hepatology*. 2010; 52:197–203. [PubMed: 20564380]
42. Ozcan U, Yilmaz E, Ozcan L, Furuhashi M, Vaillancourt E, Smith RO, Gorgun CZ, et al. Chemical chaperones reduce ER stress and restore glucose homeostasis in a mouse model of type 2 diabetes. *Science*. 2006; 313:1137–1140. [PubMed: 16931765]
43. Lindor KD, Kowdley KV, Heathcote EJ, Harrison ME, Jorgensen R, Angulo P, Lymp JF, et al. Ursodeoxycholic acid for treatment of nonalcoholic steatohepatitis: results of a randomized trial. *Hepatology*. 2004; 39:770–778. [PubMed: 14999696]
44. Leuschner UF, Lindenthal B, Herrmann G, Arnold JC, Rossle M, Cordes HJ, Zeuzem S, et al. High-dose ursodeoxycholic acid therapy for nonalcoholic steatohepatitis: a double-blind, randomized, placebo-controlled trial. *Hepatology*. 2010; 52:472–479. [PubMed: 20683947]
45. Hallen S, Fryklund J, Sachs G. Inhibition of the human sodium/bile acid cotransporters by site-specific methanethiosulfonate sulfhydryl reagents: substrate-controlled accessibility of site of inactivation. *Biochemistry*. 2000; 39:6743–6750. [PubMed: 10828993]
46. Bonge H, Hallen S, Fryklund J, Sjoström JE. Cytostar-T scintillating microplate assay for measurement of sodium-dependent bile acid uptake in transfected HEK-293 cells. *Analytical biochemistry*. 2000; 282:94–101. [PubMed: 10860504]
47. Hov JR, Keitel V, Laerdahl JK, Spomer L, Ellinghaus E, ElSharawy A, Melum E, et al. Mutational characterization of the bile acid receptor TGR5 in primary sclerosing cholangitis. *PloS one*. 2010; 5:e12403. [PubMed: 20811628]
48. Chen W, Owsley E, Yang Y, Stroup D, Chiang JY. Nuclear receptor-mediated repression of human cholesterol 7 α -hydroxylase gene transcription by bile acids. *Journal of lipid research*. 2001; 42:1402–1412. [PubMed: 11518759]

49. Stiles B, Wang Y, Stahl A, Bassilian S, Lee WP, Kim YJ, Sherwin R, et al. Live-specific deletion of negative regulator Pten results in fatty liver and insulin hypersensitivity. *Proc Natl Acad Sci U S A*. 2004; 101:2082–2087. [PubMed: 14769918]
50. Wu Q, Kazantzis M, Doege H, Ortegon AM, Tsang B, Falcon A, Stahl A. Fatty acid transport protein 1 is required for nonshivering thermogenesis in brown adipose tissue. *Diabetes*. 2006; 55:3229–3237. [PubMed: 17130465]

Cholic Acid



Taurocholic Acid

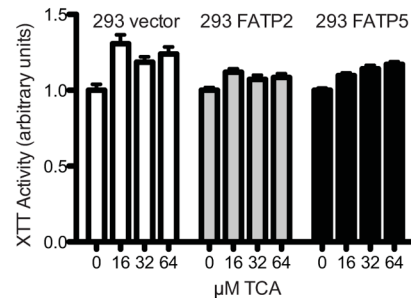
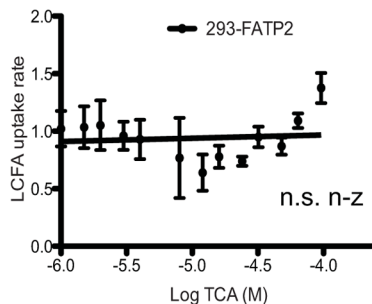
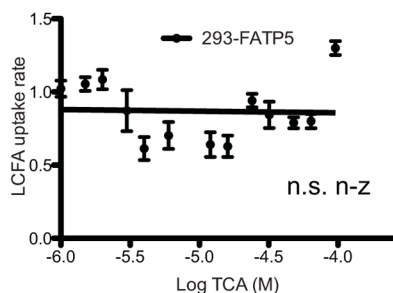


Figure 1. Inhibition of hepatic FATPs by primary bile acids

Uptake assays with stable cell lines were done as shown in Sup. Fig. 1A. Normalized LCFA uptake rates (in arbitrary units) by FATP5 (first column) and FATP2 (second column) expressing cells are plotted against the indicated bile acids (in log M). Toxicity of each bile acid was tested against all three stable cell lines (column 3) using XTT assays. Lines show either non-linear or linear regression through data points. IC₅₀ for non-linear regressions are shown in Tab. 1. N.s. n-z (not statistical non-zero) and * (p<0.05) ** (p<0.01) indicate whether the linear regression slopes differ significantly from zero.

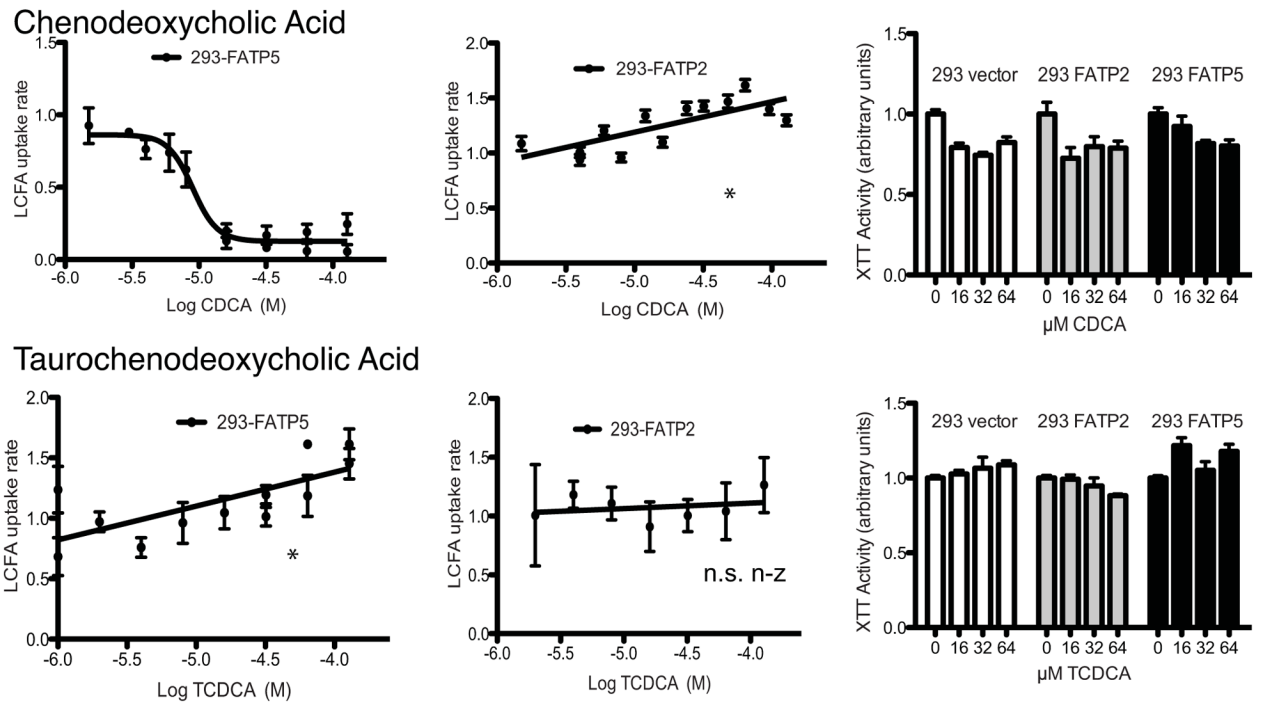


Figure 2. Inhibition of hepatic FATPs by primary bile acids
 Experiments were performed and analyzed as for Fig. 1.

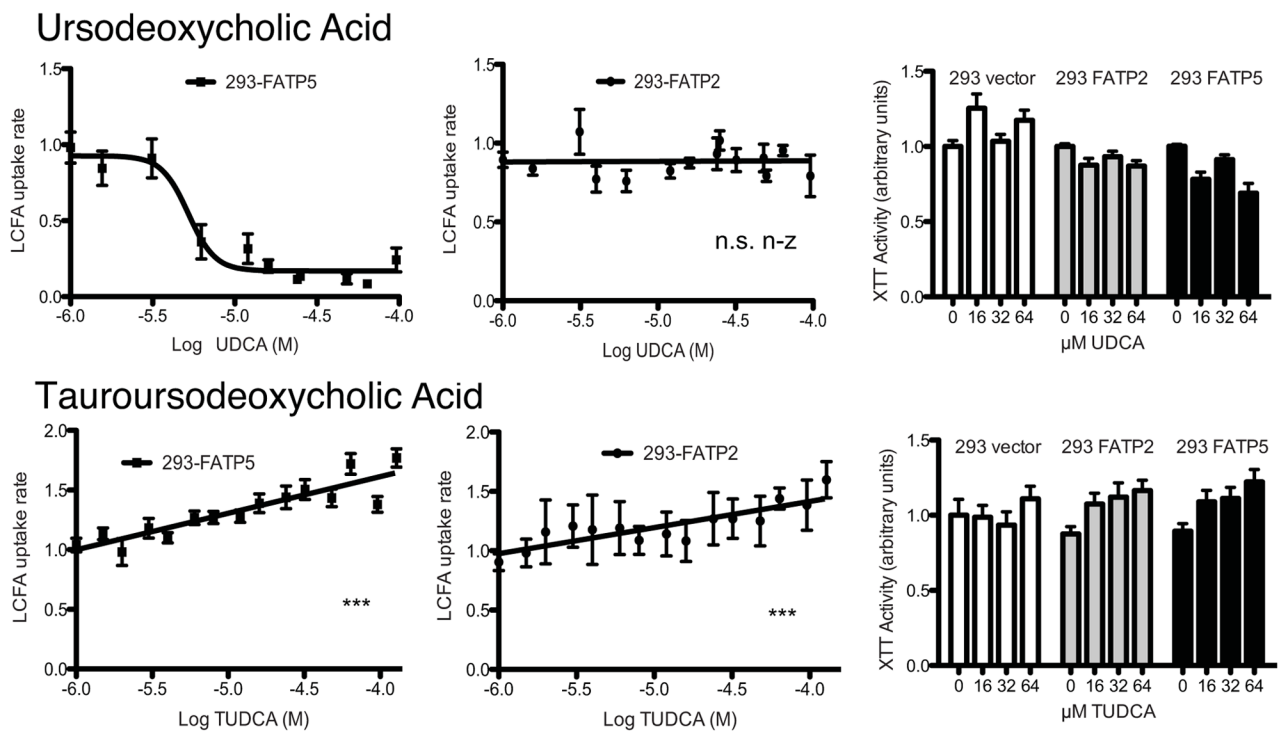


Figure 3. Inhibition of hepatic FATPs by secondary bile acids

Normalized LCFA uptake rates (in arbitrary units) by FATP5 (first column) and FATP2 (second column) expressing cells are plotted against the indicated bile acids (in log M). Toxicity of each bile acid was tested against three stable cell lines (column 3) using XTT assays. Lines show either non-linear or linear regression through data points. IC_{50} for non-linear regressions are shown in Tab. 1. N.s. n-z (not statistical non-zero) and *** ($p < 0.001$) indicate whether the linear regression slopes differ significantly from zero.

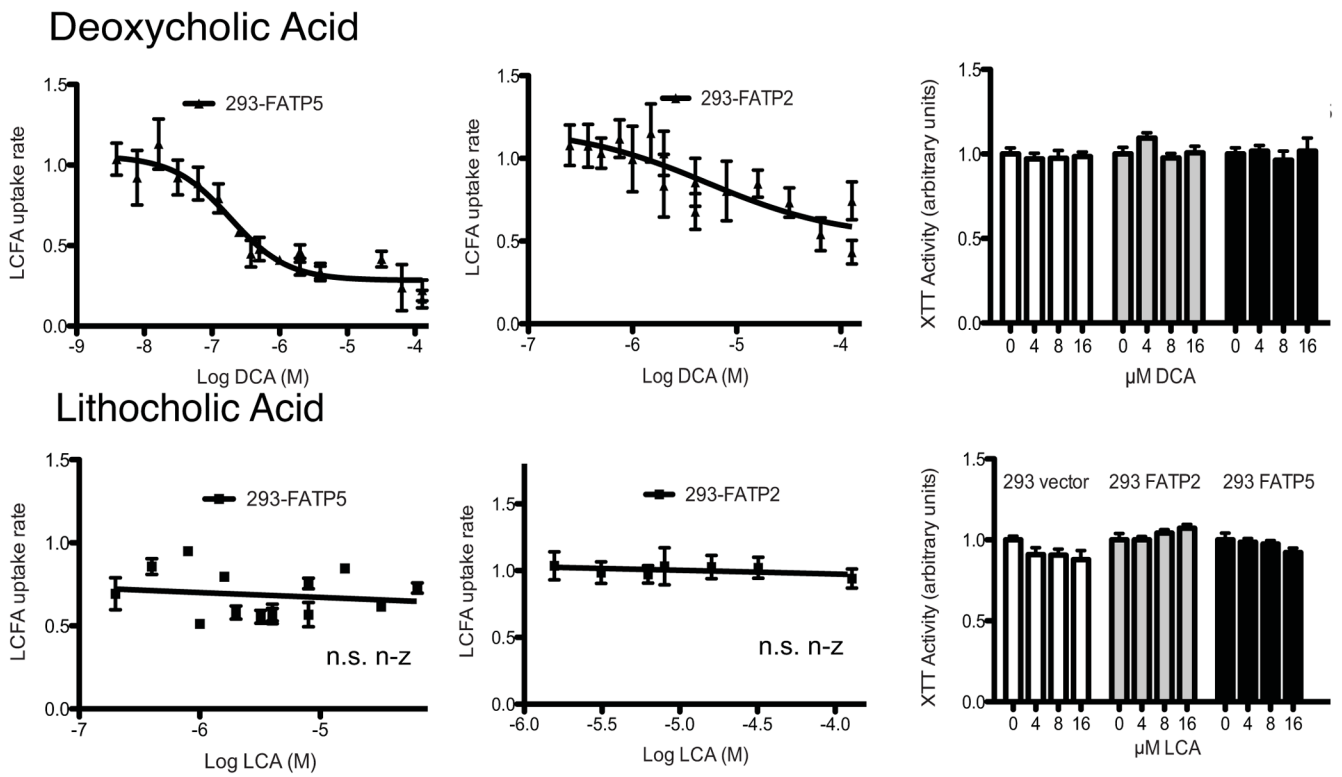


Figure 4. Inhibition of hepatic FATPs by secondary bile acids
 Experiments were performed and analyzed as for Fig. 3.

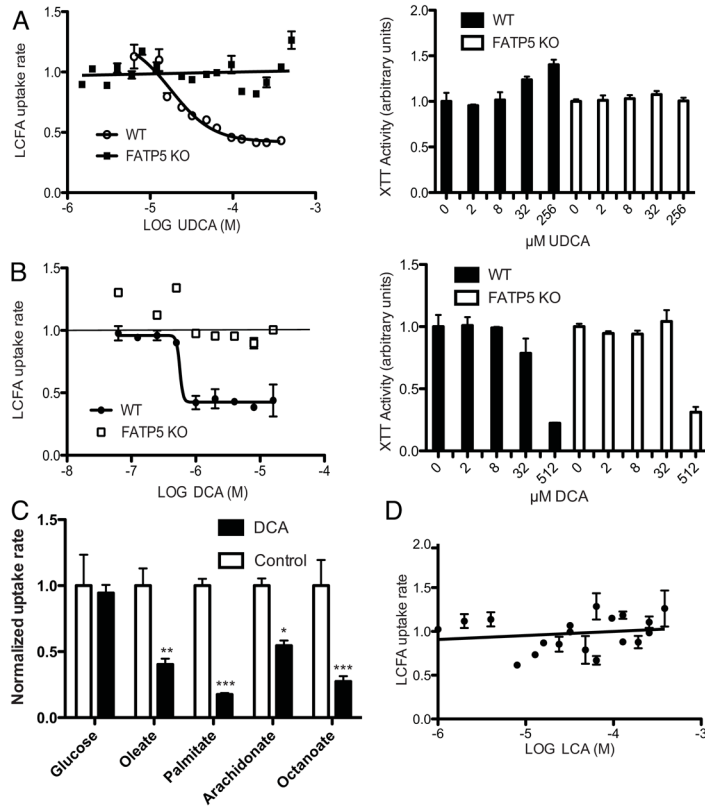


Figure 5. Ex vivo inhibition of hepatic LCFA uptake by UDCA and DCA

Quencher based LCFA uptake assay (in arbitrary units) with mouse primary hepatocytes from FATP5 wild-type (WT, circles) or knockout (FATP5 KO, squares) in 24 well plates exposed to the indicated bile acids (log M) for 2 hours during assay. A) (left) The lines show a non-linear regression through the WT data points and linear regression through the FATP5 KO data points. (right) XTT determined viability of primary mouse hepatocytes after 48 hour UDCA treatment. B) (left) The lines show a non-linear regression through the WT data, horizontal line indicates basal uptake rate. (right) XTT determined viability of primary mouse hepatocytes after 48 hour DCA treatment. C) Uptake assays with the indicated ¹⁴C-radiolabeled fatty acids and a 2-deoxy-D[³H]glucose/glucose mix were performed with primary hepatocytes as shown in Sup. Fig. 6 for oleate. For comparison of the DCA effect across substrates, data were normalized to untreated controls. D) The line shows a non-linear regression through the WT data points.

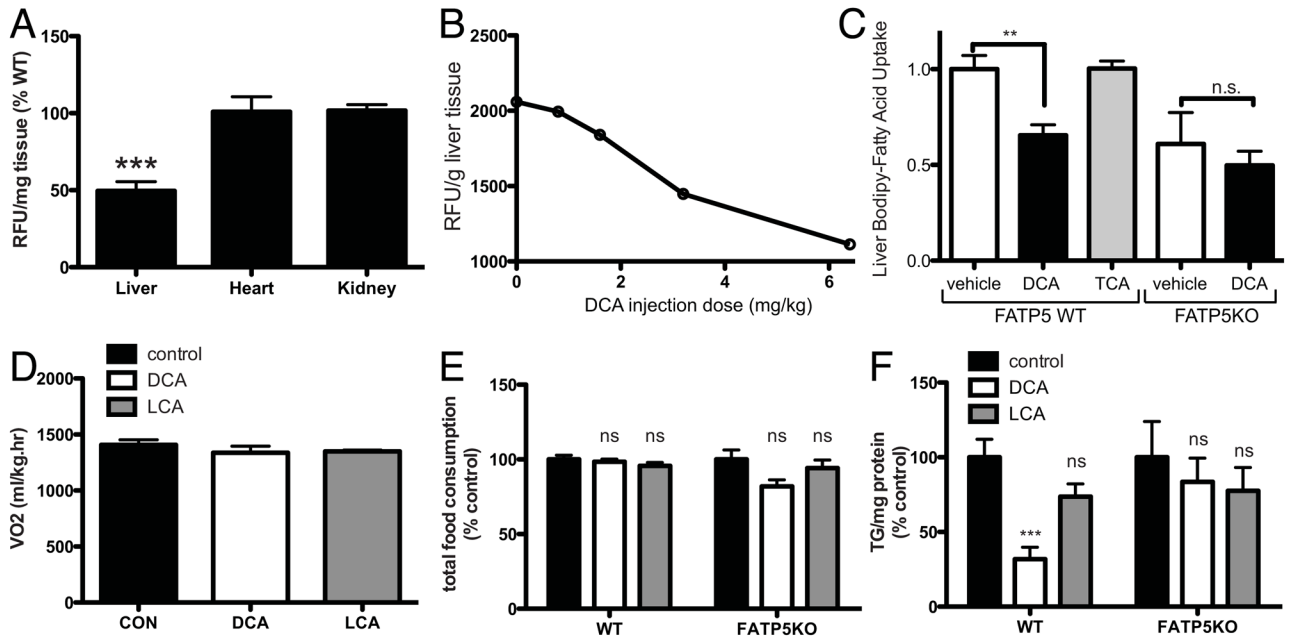


Figure 6. FATP5 dependent reduction of hepatic LCFA uptake by DCA

A) Validation of the non-radioactive hepatic LCFA uptake assay *in vivo* using WT and FATP5 KO mice. Comparison of hepatic LCFA uptake by wild-type and FATP5KO animals following injection with BSA-bound fluorescent LCFA compound. 20 min post injection fluorescence in organic extracts from the indicated tissues was determined, normalized to tissue weight and expressed as % of wild-type (see Materials and Methods). B) Acute reduction of hepatic LCFA uptake after two *i.p.* injections of DCA or DMSO following 20 μ M of BSA-bound fluorescent LCFA analog C1-BODIPY-C12. C) Acute effects of injecting 6.4mg/kg body weight DCA or TCA into WT or FATP5KO mice on hepatic LCFA uptake rates (data from three independent experiments). D) Chronic DCA/LCA injection. FATP5 WT and null animals were injected daily subcutaneously with 3.2mg/kg body weight DCA (white bars), LCA (grey bars) or DMSO (control, black bars) for 47 days. CO₂ production rates were determined using metabolic chambers. At the end of the treatment, cumulative high fat food consumption (E) and the TAG contents in livers were determined (F). ns: $p>0.05$, * $p<0.05$, *** $p<0.001$.

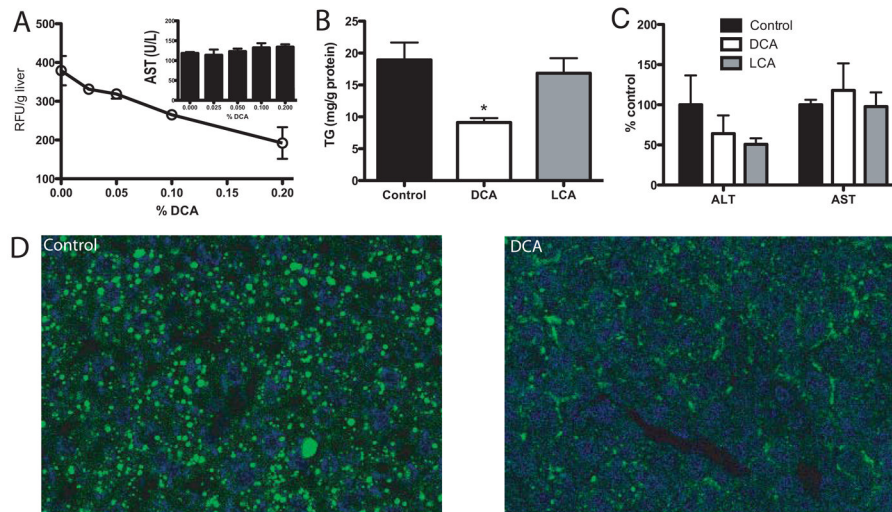


Figure 7. Effects of DCA supplementation on liver physiology

A) Mice were fed with the indicated concentrations of DCA added to high-fat food for 1 week followed by i.p. injection with 100 μ l of a 20 μ M solution of the fluorescent LCFA analog C₁-BODIPY-C₁₂ bound to BSA. 40 minutes post injection livers were removed, solvent extracted and fluorescence at 515 nm was determined. The insert shows serum AST levels after 1 week of DCA/high-fat food feeding. B–D) WT animals were fed high fat food supplemented with 0.5mg/g DCA (white bars), 0.5mg/g LCA (grey bars) or non-supplemented high fat chow for 49 days. After the treatments, the TAG in livers (B) and serum transaminase activity (C) was determined. D) Assessment of neutral lipid accumulation by confocal microscopy imaging of bodipy-stained neutral lipids in liver sections from DCA and control animals.

Table 1

Data summary for FATP5 and FATP2 inhibitors.

Bile Acid/Compound	IC50 FATP5	IC50 FATP2	Physiological Concentration(μM)	Reversible Inhibition
CA	31 μ M	/	0.135[22]–0.308[23]	Yes
TCA	/	/	0.105(0.021–0.433)[23]	/
CDCA	10 μ M	/	0.205[22]–0.502[23]	Yes
TCDC	/	/	0.232(0.022–0.621)[23]	/
THCA	/	/		/
UDCA	5 μ M	/	0.054[23]	Yes
TUDCA	/	/	0.004[23]	/
DCA	0.19 μ M	5 μ M	0.133[22]–0.415[23]	Yes
LCA	/	/	0.012 [22]–0.057[23]	/
CB-2	/	8 μ M	/	Yes
CB-5	7 μ M (tox)	18 μ M (tox)	/	No (tox)
CB-6	38 μ M	16 μ M	/	No